Double upscaling procedure for the Sine-Gordon equation with highly-oscillating coefficients: homogenization and modulation equations

Sergey L. Gavrilyuk, Bruno Lombard

Double upscaling procedure for the Sine-Gordon equation with highly-oscillating coefficients: homogenization and modulation equations

Sergey Gavrilyuk[a], Bruno Lombard[b,*]

[a] *Aix Marseille Univ, CNRS, IUSTI UMR 7343, Marseille, France*
[b] *Aix Marseille Univ, CNRS, Centrale Marseille, LMA UMR 7031, Marseille, France*

Abstract

We study the sine-Gordon equation with h-periodic in space coefficients. Leading-order homogenization yields an effective sine-Gordon equation for which travelling wave periodic solutions of wavelength $\lambda \gg h$ can be determined. The periodic solutions are then modulated on a scale $\Lambda \gg \lambda$. As we know, the corresponding Whitham equations are elliptic, which ensures that the periodic solution is unstable. However, the instability scenarios are not universal. In this paper, such scenarios are described both in the low and high energy regimes and for supersonic compared to the averaged sound speed case. In the low energy case the space derivatives of the solutions "explode" in finite time (a caustic appears), while in the high energy case the solutions grow almost linearly in time.

Keywords: Two-scale homogenization, nonlinear waves, Whitham method, modulation equations.

Contents

*Corresponding author. Tel.: +33 491 84 52 42 53.
Email addresses: sergey.gavrilyuk@univ-amu.fr (Sergey Gavrilyuk), lombard@lma.cnrs-mrs.fr (Bruno Lombard)

1. Introduction

We often encounter applications in which the physical parameters vary on a scale h much smaller than a characteristic wavelength λ. It is the paradigm of *homogenization*, initiated in the 70's and which intervenes in many areas of applied sciences, such as solid mechanics and photonics which allows us to determine "effective" parameters of such a media. The aim of homogenization is to replace a partial differential equation (PDE) with highly oscillating coefficients by a PDE with constant effective coefficients. Doing so is very advantageous, both from theoretical and numerical points of view. A bibliographic review of homogenization is out of our scope. We only refer the interested reader to [3] for a rigorous presentation of the two-scale asymptotic method for elliptic equations with periodic coefficients, and to [4] for linear wave equations. Litterature on homogenization of nonlinear wave equations with oscillating coefficients is more sparse. Theoretical issues are found in [11], and the propagation of nonlinear elastic waves in a finely layered medium is numerically investigated in [24].

Another well known upscaling method was developed by Whitham [28, 29]. Assuming a modulational length Λ much greater than wavelength λ of periodic travelling waves, the Whitham modulation equations emerge as the Euler-Lagrange equations for the corresponding averaged Lagrangian. Again, a bibliographic review of Whitham's method is out of our scope (for this, we refer to the monographs [29, 21, 9]). A general approach for the study of modulation equations for a large class of Hamiltonian systems can be found in [8]. A connection between the predictions of Whitham theory and the rigorous spectral theory have been stressed in [19]. In particular, the Whitham modulation equations appeared to be a powerful method in the study of the dispersive shocks as the solutions of the Gurevich-Pitaevskii problem (the Riemann problem for dispersive equations) [18, 17, 15, 5, 16] and references therein.

Adressing simultaneously the three spatial scales, with

$$h \ll \lambda \ll \Lambda \tag{1}$$

is less usual. To investigate the interplay of the three scales (1) on nonlinear waves, we focus on the celebrated sine-Gordon equation

$$\rho(x)\, u_{tt} - \left(E(x)\, u_x\right)_x + \gamma(x) \sin u = 0 \tag{2}$$

with variable coefficients ρ, E and γ. The general form of (2) with constant coefficient $\rho = E = \gamma \equiv 1$ constitutes one of the simplest and most widely applied prototypes of nonlinear wave equations in mathematical physics. It appeared originally in 1862 in the study of the

geometry of surfaces with negative Gaussian curvature, e.g. an hyperboloid. Since then, this equation has been involed in many physical contexts, such as the physics of particles, the crystal dislocations, the propagation of magnetic flux on a Josephson lines, the dynamics of DNA, and the oscillations of a series of rigid pendula attached to a stretched rubber band, to cite a few examples. The interested reader is referred to the monograph [12] for more background and physical applications.

To the best of our knowledge, homogenization of the sine-Gordon with oscillating coefficients (2) (i.e. the upscaling $h \to \lambda$) has not been adressed. On the contrary, some works have tackled with the modulation equations (i.e. the upscaling $\lambda \to \Lambda$) of sine-Gordon and related equations. In [20], the spectral stability of periodic travelling waves of the nonlinear Klein-Gordon equation is investigated. In [13], existence of a gradient catastrophe is proven, and the behavior of solutions to the related focusing nonlinear Schrödinger equation near this point is addressed through the hodograph transform. In a series of works [22, 23], Whitham modulation equations of sine-Gordon equation are interpreted as equations of hydrodynamics with a finite-time singularity.

Our contribution is as follows. Section 2 concerns the homogenization of sine-Gordon equations with periodic coefficients by using its variational formulation. At leading order, the homogenized equation is the sine-Gordon equation with effective constant coefficients. Section 3 deals with the construction of a periodic solution to the effective sine-Gordon in the supersonic case. A constructive algorithm is proposed, useful for forthcoming numerical simulations. Section 4 studies the modulation equations in the limit of small oscillation amplitudes. The scenario of instability (time of occurence of a singularity, behavior near the caustics) is fully described. Section 5 illustrates numerically the findings, both about homogenization and modulational instability. Lastly, Section 6 proposes future directions of research.

2. Homogenization

2.1. Periodic medium

We consider the 1D sine-Gordon equation with h-periodic coefficients

$$\rho_h(x)\,\partial_t^2 u_h - \partial_x\left(E_h(x)\partial_x u_h\right) + \gamma_h(x)\,\sin u_h = 0. \tag{3}$$

In elasticity, ρ_h and E_h evocate density and Young's modulus, respectively, and γ_h is a nonlinear parameter. Equation (3) emerges from the stationarity of the action a_h, with Lagrangian $\mathcal{L}_h$ and potential V_h:

$$\left|\begin{array}{l} a_h = \displaystyle\int_{t_0}^{t_1}\int_{-\infty}^{+\infty} \mathcal{L}_h\, dt\, dx, \\ \mathcal{L}_h = \rho_h\left(x\right)\dfrac{u_{h,t}^2}{2} - E_h(x)\dfrac{u_{h,x}^2}{2} - V_h\left(u_h, x\right), \\ V_h = \gamma_h(x)(1-\cos u_h). \end{array}\right. \tag{4}$$

The oscillating coefficients are written $\rho_h(x) = \rho(x/h)$, $E_h(x) = E(x/h)$ and $\gamma_h(x) = \gamma(x/h)$, where

$$(\rho,\, E,\, \gamma) \in L^\infty_{per}(0,1) := \left\{g \in L^\infty(\mathbb{R}),\, g(y+1) = g(y), a.e.\, y \in \mathbb{R}\right\},$$

with $\rho \geq \rho_{\min} > 0$ and $E \geq E_{\min} > 0$.

2.2. Averaging

A fast scale $y = x/h$ is introduced, and separation of scale is assumed so that x and y are independant variables. The following ansatz is used:

$$u_h = \overline{u}(t,x) + h\,\tilde{u}(t,x,y) + o(h), \tag{5}$$

with 1–periodic function $\tilde{u}(t,x,\bullet)$. As customary in this two-scale analysis, partial differentiation with respect to x has to be rewritten as $\partial_x + \frac{1}{h}\partial_y$. Injecting (5) into (4) yields

$$\mathcal{L}_h = \rho(y)\frac{\overline{u}_t^2}{2} - E\,(y)\,\frac{(\overline{u}_x + \tilde{u}_y)^2}{2} - V\,(\overline{u}, y) + \mathcal{O}(h). \tag{6}$$

This Lagrangian is now averaged on the fast scale

$$\mathcal{L}_0 := \overline{\mathcal{L}_h} = \int_0^1 \left(\rho\,(y)\,\frac{\overline{u}_t^2}{2} - E\,(y)\,\frac{(\overline{u}_x + \tilde{u}_y)^2}{2} - V\,(\overline{u}, y)\right) dy + \mathcal{O}(h). \tag{7}$$

The variation of $\mathcal{L}_0$ with respect to $\tilde{u}$ gives

$$(E(y)(\overline{u}_x + \tilde{u}_y))_y = 0. \tag{8}$$

It implies

$$E(y)(\overline{u}_x + \tilde{u}_y) = A(t,x), \tag{9}$$

where A does not depend on y, and thus

$$\overline{u}_x + \tilde{u}_y = \frac{A(t,x)}{E(y)}. \tag{10}$$

Since $\tilde{u}$ is periodic with respect to y and $\overline{u}$ does not depend on y, one has:

$$\overline{u}_x = A(t,x)\int_0^1 \frac{dy}{E(y)}. \tag{11}$$

Finally, one obtains

$$\overline{u}_x + \tilde{u}_y = \frac{\overline{u}_x}{E(y)\displaystyle\int_0^1 \frac{ds}{E(s)}}. \tag{12}$$

The averaged Lagrangian becomes then

$$\mathcal{L}_0 = \rho_0\frac{\overline{u}_t^2}{2} - E_0\frac{\overline{u}_x^2}{2} - V_0(\overline{u}) + \mathcal{O}(h), \tag{13}$$

with

$$\rho_0 = \int_0^1 \rho(y)dy, \quad E_0 = \left(\int_0^1 \frac{dy}{E(y)}\right)^{-1}, \quad V_0(\overline{u}) = \int_0^1 V(\overline{u}, y)dy. \tag{14}$$

In the case of the sine-Gordon equation, $V_0(\overline{u}) = \gamma_0(1 - \cos(\overline{u}))$, with $\gamma_0 = \int_0^1 \gamma(y)dy$. The Euler-Lagrange equations on (13) finally leads to

$$\rho_0\,\partial_t^2 u_0 - E_0\,\partial_x^2 u_0 + \gamma_0\,\sin u_0 = 0, \tag{15}$$

with $u_0 = \overline{u}$ and canceling the $\mathcal{O}(h)$ term. At leading order, the homogenized sine-Gordon equation thus maintains the structure of the original equation (3), simply changing the oscillating coefficients by effective coefficients. One recognizes the arithmetic and geometric averages of ρ and E, respectively, as in linear elastodynamics [27]. It is emphasized that the averaging procedure is valid whatever the potential V, enabling generalizations e.g. to the nonlinear Klein-Gordon equation.

In practice, the effective linear sound speed $c_0 = \sqrt{E_0/\rho_0}$ can be much smaller than the minimal sound speed in the microstructured medium. As a simple example, we consider a periodic mixture of two components (denoted by A and B) with parameters ρ_i, E_i, $i = A, B$, assembled periodically with a geometric ratio $0 < \alpha < 1$. The effective coefficients (14) lead to

$$\frac{1}{c_0^2} = (\alpha\rho_A + (1-\alpha)\rho_B)\left(\frac{\alpha}{E_A} + \frac{1-\alpha}{E_B}\right). \tag{16}$$

Usually, if $\rho_A > \rho_B$ then $E_A > E_B$. Consequently, there exists a maximum of $1/c_0^2$, i.e. c_0^2 attains its minimum at the critical point

$$\alpha_c = \frac{(\rho_B - \rho_A)/E_B + (1/E_B - 1/E_A)\rho_B}{2(\rho_A - \rho_B)(1/E_A - 1/E_B)}. \tag{17}$$

Let us consider a numerical example, with $\rho_A = 1$, $\rho_B = 100$, $E_A = 1$, $E_B = 100$. Then $\alpha_c = 0.5$ and $c_0^2 \approx 0.0392 \ll 1 = \min(c_A^2, c_B^2)$. Such a drastical decrease of the effective speed is one of the physical features of heterogeneous media.

3. Periodic waves in the homogenized medium

Based on the homogenization performed in Section 2, we leave out the microstructure and consider the sine-Gordon equation with constant coefficients.

3.1. Supersonic periodic solution

Passing to scaled independent variables denoted with sign 'tilde': $x = \sqrt{E_0/\gamma_0}\ \tilde{x}$, $t = \sqrt{\rho_0/\gamma_0}\ \tilde{t}$ and suppressing in the following the tilde and the index 0 in (15), one obtains the standard sine-Gordon equation

$$u_{tt} - u_{xx} + \sin u = 0. \tag{18}$$

It follows from the adimentionalized Lagrangian

$$\mathcal{L}_0 = \frac{u_t^2}{2} - \frac{u_x^2}{2} + V(u), \qquad V(u) = 1 - \cos u. \tag{19}$$

Now, we consider travelling wave solutions of (18). Let $\xi = x - Dt$ be the coordinates in the moving frame, where D is the constant wave velocity. Since the effective sound velocity can be very small, we will concentrate only on supersonic solution $D > 1$ as the physical ones. Denoting by 'prime' the derivative with respect to ξ, one obtains

$$(D^2 - 1)\frac{u'^2}{2} + V(u) = \mathcal{E}, \tag{20}$$

where the density of energy $\mathcal{E}$ is a constant. The graph of the potential $V(u)$ is shown in Figure 1. We denote $\pm\theta_0(\mathcal{E})$, with $-\pi < -\theta_0 \leq 0 \leq \theta_0 < \pi$, the two roots of the equation

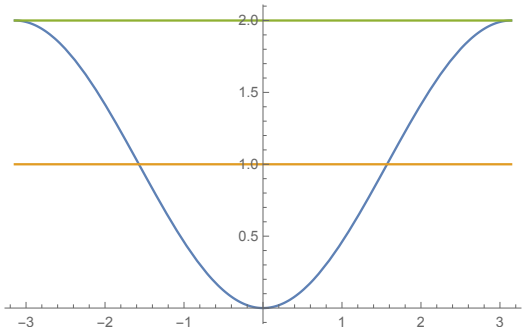

Figure 1: The potential $V(u) = 1 - \cos(u)$ is shown on the interval $[-\pi, \pi]$. The horizontal orange line denotes the energy $\mathcal{E} = 1$.

$$1 - \mathcal{E} = \cos\theta_0, \quad 0 < \mathcal{E} < 2. \tag{21}$$

The solution $-\theta_0 < u(\xi) < \theta_0$ is deduced:

$$\int_{-\theta_0}^{u} \frac{d\theta}{\sqrt{\cos\theta - \cos\theta_0}} = \pm\sqrt{\frac{2}{D^2 - 1}}\,(\xi + \xi_0), \quad \xi_0 = const.$$

Introducing the incomplete elliptic integral of the first kind [1]:

$$F(\phi, m) = \int_0^{\phi} \frac{d\theta}{\sqrt{1 - m\sin^2\theta}},$$

one obtains

$$\int_{-\theta_0}^{u} \frac{d\theta}{\sqrt{\cos\theta - \cos\theta_0}} = \frac{2}{\sqrt{1 - \cos\theta_0}} \left(F\left(\frac{u}{2}, m\right) + F\left(\frac{\theta_0}{2}, m\right)\right),$$

with

$$m = \frac{1}{\sin^2\left(\frac{\theta_0}{2}\right)}.$$

Consequently, the periodic solution $-\theta_0 < u < \theta_0$ can be found implicitly from:

$$\frac{2}{\sqrt{1 - \cos\theta_0}} \left(F\left(\frac{u}{2}, m\right) + F\left(\frac{\theta_0}{2}, m\right)\right) = \pm\sqrt{\frac{2}{D^2 - 1}}\,(\xi + \xi_0),$$

where ξ_0 is a constant, or equivalently

$$F\left(\frac{u}{2}, m\right) + F\left(\frac{\theta_0}{2}, m\right) = \pm\frac{\xi + \xi_0}{\sqrt{m(D^2 - 1)}}. \tag{22}$$

3.2. Construction of the supersonic periodic travelling wave

Based on (22), the following algorithm describes the construction of a periodic supersonic solution:

1. Without loss of generality, one takes $\xi_0 = 0$;

2. Choose the value of $0 < \mathcal{E} < 2$ and find the positive root θ_0 of (21). Take $m = 1/\sin^2\left(\frac{\theta_0}{2}\right)$;

3. Choose the supersonic wave velocity $D > 1$;

4. For $-\theta_0 < s < \theta_0$, one selects

$$\xi^+(s) = \sqrt{m(D^2-1)}\,(F(s/2,m) + F(\theta_0/2,m))\,, \quad u^+(s) = +s,$$

The graph (ξ, u) is thus defined in the interval $\xi \in (0, \lambda/2)$, where the half wavelength is given by $\lambda/2 = \xi^+(\theta_0)$.

To construct the solution in the interval $\xi \in (\lambda/2, \lambda)$, the following parametric form is used: for $-\theta_0 < s < \theta_0$, one takes

$$\xi^-(s) = \lambda/2 + \sqrt{m(D^2-1)}\,(F(s/2,m) + F(\theta_0/2,m))\,, \quad u^-(s) = -s.$$

The solution is thus constructed on the interval $(0, \lambda)$. The period λ is given by

$$\lambda = 4K\,(\mathcal{E}/2)\,\sqrt{D^2-1}, \tag{23}$$

where

$$K\,(m) = F\left(\frac{\pi}{2}, m\right) = \int_0^{\frac{\pi}{2}} \frac{d\theta}{\sqrt{1 - m\,\sin^2\theta}} \tag{24}$$

is the complete elliptic integral of the first kind. The evolution of wavelength and amplitude with $\mathcal{E}$ is illustrated in Figure 2.

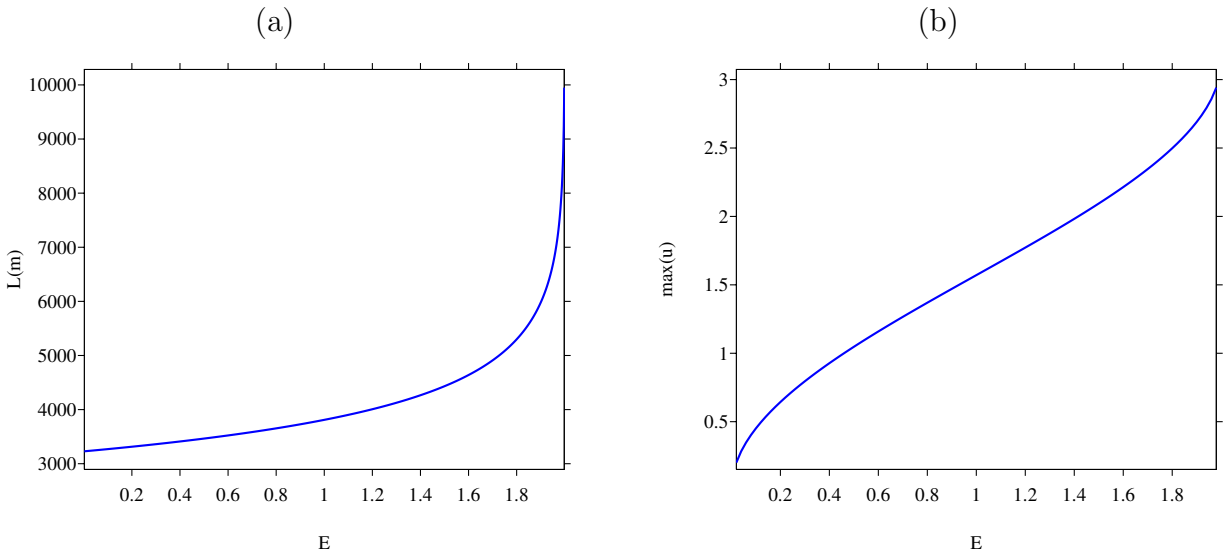

Figure 2: Evolution of the wavelength λ (a) and amplitude of u (b) with respect to the energy $\mathcal{E}$.

3.3. Generation by boundary conditions

For numerical simulations proposed in Section 5, one needs as initial data not only $u(0,x)$ but also $u_t(0,x)$. For this purpose, a convenient way is to generate periodic solutions by boundary conditions. The step 4 of the algorithm given in Section 3.2 needs to be modified. At $x=0$ and for $-\theta_0 < s < \theta_0$, the boundary condition is sought in the following parametric form:

$$t^+(s) = \frac{1}{D}\sqrt{m(D^2-1)}\,(F(s/2,m)+F(\theta_0/2,m))\,, \quad u^+(s)=s,$$

The solution u as a function of t is thus defined implicitly in the interval $t\in(0,\tau/2)$, where the half period is given by $\tau/2 = t^+(\theta_0)$. To build the solution in the interval $t\in(\tau/2,\tau)$, the following parametric form is used: for $-\theta_0 < s < \theta_0$, one takes

$$t^-(s) = t^+(\theta_0) + \frac{1}{D}\sqrt{m(D^2-1)}\,(F(s/2,m)+F(\theta_0/2,m))\,, \quad u^-(s)=-s.$$

The solution is thus defined on the interval $(0,\tau)$, $\tau=\lambda/D$. This algorithm is repeated on the interval $(\tau,2\tau)$, etc. Once u is determined, an estimate of u_t is obtained by finite differences.

4. Modulation theory

4.1. Whitham's method

In Section 3, a periodic solution with constant D and $\mathcal{E}$ of the homogenized sine-Gordon equation (18) was built. It was characterized by a wavelength λ and a phase $\theta=\omega t - kx$, where $\omega=2\pi/\tau$ is the angular frequency and $k=2\pi/\lambda$ is the wavenumber.

Now, we consider a periodic wave train with slow evolution of the parameters on a spatial scale $\Lambda \gg \lambda$. Slow variables are introduced:

$$\mu = \frac{\lambda}{\Lambda} \ll 1, \qquad X=\mu\,x, \qquad T=\mu\,t, \qquad \Theta = \omega T - kX = \mu\,\theta, \tag{25}$$

hence $\omega = -\theta_t = -\Theta_T$ and $k=\theta_x=\Theta_X$. We are looking for solutions of the form

$$u = U(\theta,T,X,\mu) = U(\theta,T,X) + \mathcal{O}(\mu). \tag{26}$$

The period of the travelling wave may be normalized to 2π, so that we impose the condition that U is 2π periodic with respect to θ. An additional averaging with respect to the fast phase θ is performed following the Whitham method [28, 29]. Using $\partial_t = \omega\,\partial_\theta + \mu\,\partial_T \approx \omega\,\partial_\theta$ and $\partial_x = -k\,\partial_\theta + \mu\,\partial_X \approx -k\,\partial_\theta$, then (19) is transformed in an ODE in θ, and the new averaged Lagrangian is

$$\overline{\mathcal{L}} = \frac{1}{2\pi}\int_0^{2\pi} \mathcal{L}_0\,d\theta \approx \frac{1}{2\pi}\int_0^{2\pi}\left(\frac{1}{2}(\omega^2-k^2)\,U_\theta^2 - V(U)\right)d\theta, \tag{27}$$

with

$$\frac{1}{2}(\omega^2-k^2)\,U_\theta^2 + V(U) = \mathcal{E} = const, \quad V(U) = 1-\cos U. \tag{28}$$

Variations of $\overline{\mathcal{L}}(\omega,k,\mathcal{E})$ with respect to θ and $\mathcal{E}$ lead to Euler-Lagrange equation and nonlinear dispersion equation, completed with a constraint of compatibility phase equation [29]:

$$(\overline{\mathcal{L}}_\omega)_T - (\overline{\mathcal{L}}_k)_X = 0, \qquad \overline{\mathcal{L}}_{\mathcal{E}} = 0, \qquad k_T + \omega_X = 0. \tag{29}$$

4.2. Modulation equations

Injecting (28) in (27) and changing the variables of integration yields

$$\begin{aligned}\overline{\mathcal{L}} &= \frac{1}{2\pi}\int_0^{2\pi}(\omega^2-k^2)\,U_\theta^2\,d\theta-\mathcal{E},\\ &= \frac{2}{2\pi}\int_{U_1(\mathcal{E})}^{U_2(\mathcal{E})}(\omega^2-k^2)\,U_\theta\,dU-\mathcal{E},\\ &= \frac{\sqrt{2\,(\omega^2-\,k^2)}}{\pi}\int_{U_1(\mathcal{E})}^{U_2(\mathcal{E})}\sqrt{\mathcal{E}-V(U)}\,dU-\mathcal{E},\end{aligned}\tag{30}$$

where $0<\mathcal{E}<2$ and $U_1<U_2$ are the roots of the equation $1-\cos U=\mathcal{E}$. The integral in (30) can be simplified:

$$\begin{aligned}\int_{U_1(\mathcal{E})}^{U_2(\mathcal{E})}\sqrt{\mathcal{E}-V(U)}\,dU &= 2\sqrt{\mathcal{E}}\int_0^{U_2(\mathcal{E})}\sqrt{1-\frac{2}{\mathcal{E}}\sin^2\frac{U}{2}}\,dU,\\ &= 4\sqrt{\mathcal{E}}\int_0^{\arcsin\sqrt{\frac{\mathcal{E}}{2}}}\sqrt{1-\frac{2}{\mathcal{E}\,\sin^2\varphi}}\,d\varphi,\\ &= 4\sqrt{\mathcal{E}}\,E\left(\arcsin\left(\sqrt{\mathcal{E}/2}\right),2/\mathcal{E}\right),\end{aligned}\tag{31}$$

with the incomplete elliptic integral of the second kind

$$E(\phi,m)=\int_0^{\phi}\sqrt{1-m\,\sin^2\theta}\,d\theta.$$

It follows the averaged Lagrangian

$$\overline{\mathcal{L}}=\sqrt{\omega^2-k^2}\,f(\mathcal{E})-\mathcal{E},\quad\text{with } f(\mathcal{E})=\frac{4\sqrt{2\,\mathcal{E}}}{\pi}E\left(\arcsin\left(\sqrt{\mathcal{E}/2}\right),2/\mathcal{E}\right).\tag{32}$$

Injecting (32) in (29) gives the modulation equations for the sine-Gordon equation [25] :

$$\begin{cases}\left(\dfrac{\omega f(\mathcal{E})}{\sqrt{\omega^2-k^2}}\right)_T+\left(\dfrac{k f(\mathcal{E})}{\sqrt{\omega^2-k^2}}\right)_X=0, & \text{(33a)}\\ \omega^2-k^2=\left(f'(\mathcal{E})\right)^{-2}, & \text{(33b)}\\ k_T+\omega_X=0. & \text{(33c)}\end{cases}$$

The function f in (32)-(33) and its derivatives can be further simplified, based on the following lemma proven in Appendix A.

Lemma 1. *The function $f(\mathcal{E})$ in (32) and its derivatives can be written in terms of complete elliptic integrals:*

$$f(\mathcal{E})=\frac{8}{\pi}\left(E\left(\mathcal{E}/2\right)-\left(1-\mathcal{E}/2\right)K\left(\mathcal{E}/2\right)\right),\qquad f'(\mathcal{E})=\frac{2}{\pi}K\left(\mathcal{E}/2\right),$$
$$f''(\mathcal{E})=\frac{1}{\pi}\frac{1}{\mathcal{E}\left(1-\mathcal{E}/2\right)}\left(E\left(\mathcal{E}/2\right)-\left(1-\mathcal{E}/2\right)K\left(\mathcal{E}/2\right)\right).$$

Moreover, the limit cases of low and high energy yield:

- $f(\mathcal{E}) \to 0,\ f'(\mathcal{E}) \to 1$ *if* $\mathcal{E} \to 0$;
- $f(\mathcal{E}) \to \dfrac{8}{\pi},\ f'(\mathcal{E}) \to +\infty$ *if* $\mathcal{E} \to 2$.

Using Lemma 1 in (33b) at low energy $\mathcal{E} \to 0$ recovers the linear dispersion relation $\omega^2 = k^2 + 1$. On the contrary, the limit-case of high energy $\mathcal{E} = 2$ gives $\omega = \pm k$, i.e. nondispersive waves.

4.3. Complex Riemann invariants

The slow evolution of $(\omega, k, \mathcal{E})$ is described by (33). Using $D = \omega/k$, equation (33b) provides

$$k = \frac{1}{\sqrt{D^2-1}}\frac{1}{f'(\mathcal{E})}, \qquad \omega = \frac{D}{\sqrt{D^2-1}}\frac{1}{f'(\mathcal{E})}.$$

Injecting this equation in (33c) and (33a) gives the system in variables $(\mathcal{E}, D)$

$$\begin{cases} \left(\dfrac{1}{\sqrt{D^2-1}}\dfrac{1}{f'(\mathcal{E})}\right)_T + \left(\dfrac{D}{\sqrt{D^2-1}}\dfrac{1}{f'(\mathcal{E})}\right)_X = 0, & \text{(34a)} \\ \left(\dfrac{D}{\sqrt{D^2-1}}f(\mathcal{E})\right)_T + \left(\dfrac{1}{\sqrt{D^2-1}}f(\mathcal{E}\right)_X = 0. & \text{(34b)} \end{cases}$$

Its quasilinear form is

$$\begin{cases} \dfrac{Df'}{f}\mathcal{E}_T - \dfrac{1}{D^2-1}D_T + \dfrac{f'}{f}\mathcal{E}_X - \dfrac{D}{D^2-1}D_X = 0, \\ f''\mathcal{E}_T + \dfrac{Df'}{D^2-1}D_T + Df''\mathcal{E}_X + \dfrac{f'}{D^2-1}D_X = 0. \end{cases} \tag{35}$$

This system is written in matrix form

$$\mathbf{A}\mathbf{U}_T + \mathbf{B}\mathbf{U}_X = \mathbf{0},$$

with

$$\mathbf{U}^\top = (\mathcal{E}, D), \quad \mathbf{A} = \begin{pmatrix} \dfrac{Df'}{f} & -\dfrac{1}{D^2-1} \\ f'' & \dfrac{Df'}{D^2-1} \end{pmatrix}, \quad \mathbf{B} = \begin{pmatrix} \dfrac{f'}{f} & -\dfrac{D}{D^2-1} \\ Df'' & \dfrac{f'}{D^2-1} \end{pmatrix}. \tag{36}$$

The eigenvalues β satisfying $\det(\mathbf{B} - \beta\mathbf{A}) = 0$ are

$$\begin{aligned} \beta &= \frac{1 + \mathrm{i}\,\alpha D}{D + \mathrm{i}\,\alpha}, \\ &= \frac{D(1+\alpha^2) + \mathrm{i}\,\alpha(D^2-1)}{D^2 + \alpha^2}, \\ &= \beta_r + \mathrm{i}\,\beta_i, \end{aligned} \tag{37}$$

and $\overline{\beta} = \beta_r - \mathrm{i}\,\beta_i$. Lemma 1 gives

$$\alpha(\mathcal{E}) = \sqrt{\frac{f''(\mathcal{E})f(\mathcal{E})}{f'^2(\mathcal{E})}} = \frac{1}{\sqrt{\mathcal{E}(2-\mathcal{E})}}\frac{2E\left(\mathcal{E}/2\right) - (2-\mathcal{E})K\left(\mathcal{E}/2\right)}{K\left(\mathcal{E}/2\right)}. \tag{38}$$

Since β is complex, the system (35) is elliptic for all $\mathcal{E}$ and D, which proves the modulation instability of the sine-Gordon equations. Now, we will find the Riemann invariants in complex form. Let $\mathbf{e}^\top = (\xi, \eta)$ be the left eigenvector satisfying:

$$\mathbf{e}^\top (\mathbf{B} - \beta \mathbf{A}) = \mathbf{0}. \tag{39}$$

The components (ξ, η) are related by:

$$\xi \frac{f'(1-\beta D)}{f} + \eta f''(D-\beta) = 0.$$

Replacing the expression of β from (37), one gets:

$$\eta = \mathrm{i} \frac{\xi}{\alpha f'}.$$

Now, let us consider the expression

$$\begin{aligned} \mathbf{e}^\top \mathbf{A}\mathbf{U}_T &= \xi \left(1, \frac{\mathrm{i}}{\alpha f'}\right) \mathbf{A}\mathbf{U}_T = \xi \frac{D+\mathrm{i}\alpha}{\alpha} \left(\sqrt{\frac{f''}{f}}, \frac{\mathrm{i}}{D^2-1}\right) \mathbf{U}_T, \\ &= \mathrm{i}\,\xi \frac{D+\mathrm{i}\alpha}{\alpha} \left(\frac{1}{D^2-1} D_T + \mathrm{i} \sqrt{\frac{f''}{f}} \mathcal{E}_T\right), \\ &= \mathrm{i}\,\xi \frac{D+\mathrm{i}\alpha}{\alpha} \left(\frac{1}{D^2-1} D_T + \mathrm{i} \frac{1}{\sqrt{8\,\mathcal{E}\,(1-\mathcal{E}/2)}} \mathcal{E}_T\right), \end{aligned} \tag{40}$$

where we have used the relation between f and f'' given in Lemma 1. Integration leads to the complex Riemann invariant r

$$\begin{aligned} r &= \int^D \frac{dp}{p^2-1} + \mathrm{i} \int^{\mathcal{E}} \frac{ds}{\sqrt{8\,s\,(1-s/2)}}, \\ &= \ln\left(\sqrt{\frac{D+1}{D-1}}\right) + \mathrm{i}\,\arcsin\left(\sqrt{\mathcal{E}/2}\right), \end{aligned} \tag{41}$$

where r satisfies the quasilinear complex equation

$$r_T + \beta\, r_X = 0. \tag{42}$$

A similar form has been obtained in [23].

4.4. Formation of a caustic

In the following, we will use the Riemann invariant r given by (41) and focus on the case of low energy $\mathcal{E}$. We introduce the change of variables (ρ, b):

$$\mathcal{E} = 2\,\rho, \qquad D = \frac{\cosh b}{\sinh b}, \tag{43}$$

where $0 < \rho < 1$ and $b > 0$. Then (41) gives

$$r = b + \mathrm{i}\,\arcsin(\sqrt{\rho}).$$

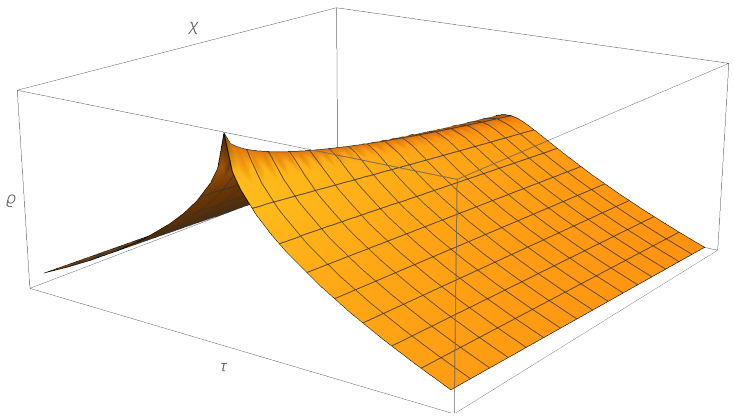

Figure 3: The graph of the function ϱ in (52) is shown. The singularity is a caustic formed at $\tau = 0$ and $\chi = 0$.

The eigenvalue β in (37) and the Riemann invariant can be simplified in the case of small ρ (i.e. small $\mathcal{E}$)

$$\beta \approx b + \mathrm{i}\frac{\sqrt{\rho}}{2}, \quad r \approx b + \mathrm{i}\sqrt{\rho}. \tag{44}$$

It follows that the eigenvalue $\beta(r)$ does not satisfy the Cauchy–Riemann conditions, and hence the eigenvalue β is not an analytic function of r. Even for holomorphic initial data, the method of characteristics thus cannot be used. Also, the life span of the solution is finite. Injecting (44) into (42) and separating the real and imaginary parts yields the system of PDEs

$$\rho_T + (\rho\, b)_X = 0, \qquad b_T + b\, b_X - \frac{1}{4}\rho_X = 0. \tag{45}$$

This is analogous to the system of shallow water equations with a negative 'gravity constant' $g = -1/4$; using this analogy, ρ is the fluid depth and b is the fluid velocity. An exact solution of (45) is known for the initial data

$$\rho(0, X) = 4a^2 \operatorname{sech}^2\left(\frac{X}{\Lambda}\right), \qquad b(0, X) = b_0, \tag{46}$$

with parameters $a > 0$, $b_0 > 0$ and $\Lambda > 0$. In comparison with [22] where $g = -1$ was considered, a factor 4 is introduced in $\rho(0, X)$ in (46) to account for $g = -1/4$. Also, we used the Galilean invariance of (45) to account for the case $b_0 \neq 0$, as required by (43). The so-called ASK solution (Akhmanov–Sukhorukov–Khokhlov) for the shallow water equations 'on the seiling' can then be written in parametric form [2, 22]: introducing the time and space parametrisation

$$T = \frac{\Lambda}{a}\frac{\xi}{(1+\xi^2)(1-\eta^2)}, \quad \frac{X}{\Lambda} = \frac{2\xi^2\eta}{(1+\xi^2)(1-\eta^2)} - \frac{1}{2}\ln\left(\frac{1+\eta}{1-\eta}\right) + \frac{b_0}{a}\frac{\xi}{(1+\xi^2)(1-\eta^2)}, \tag{47}$$

one gets

$$\rho(\xi, \eta) = 4\, a^2(1+\xi^2)(1-\eta^2), \quad b(\xi, \eta) = 2\, a\, \xi\, \eta + b_0. \tag{48}$$

Here $\xi > 0$ and $-1 < \eta < 1$. The time and space derivatives can be expressed as

$$\rho_X = \frac{-\rho_\xi T_\eta + \rho_\eta T_\xi}{J_1}, \qquad b_X = \frac{-b_\xi T_\eta + b_\eta T_\xi}{J_1},$$
$$\rho_T = \frac{\rho_\xi X_\eta - \rho_\eta X_\xi}{J_1}, \qquad b_T = \frac{b_\xi X_\eta - b_\eta X_\xi}{J_1},$$

with

$$J_1 = \det \begin{pmatrix} T_\xi & T_\eta \\ X_\xi & X_\eta \end{pmatrix} = \frac{\Lambda^2}{a} \frac{(\xi^2-1)^2 + \eta^2(-1+6\,\xi^2+3\,\xi^4)}{(-1+\eta^2)^3(1+\xi^2)^3}.$$

The Jacobian J_1 is singular when $\xi := \xi_c = 1$ and $\eta := \eta_c = 0$. In variables (T, X), it corresponds to

$$T := T_c = \frac{\Lambda}{2a}, \quad X := X_c = \frac{b_0\Lambda}{2a}. \tag{49}$$

The corresponding values of b and ρ are

$$\rho = \rho_c = 8a^2, \quad b = b_c = b_0. \tag{50}$$

Let us derive the asymptotic behavior of the solution at the vicinity of this critical point. Developing into Taylor series, one gets:

$$\chi := \frac{X - X_c}{\Lambda} \approx \eta\,(\xi - 1) + \frac{b_0}{2a}\tau, \quad \tau := \frac{T - T_c}{T_c} \approx \eta^2 - \frac{(\xi-1)^2}{2},$$
$$\varrho = \frac{\rho - 8a^2}{8a^2} \approx \xi - 1 - \left(\eta^2 - \frac{(\xi-1)^2}{2}\right).$$

It implies a biquadratic equation for $\varrho + \tau$:

$$(\varrho+\tau)^4 + 2\,\tau(\varrho+\tau)^2 - 2\left(\chi - \frac{b_0}{2a}\tau\right)^2 = 0. \tag{51}$$

The solution is

$$\varrho = -\tau - \sqrt{\sqrt{\tau^2 + 2\left(\chi - \frac{b_0}{2a}\tau\right)^2} - \tau}. \tag{52}$$

The graph of this function is shown in Figure 3 and shows the formation of a caustic.

5. Numerical results

5.1. Homogenization

Set-up. To illustrate the leading-order homogenization, one considers a uniform mesh size Δx and time step Δt. The numerical resolution of (15) is based on a finite-difference scheme, centered in space and explicit in time. This second-order scheme is stable under the CFL condition $\zeta = \max(c)\Delta t/\Delta x \leq 1$; in practice we use $\zeta = 0.95$. The scheme preserves the discrete energy. No care is taken concerning the boundaries of the computational domain, since the simulations are stopped before the wave reaches the edges. Some additional care is required for the numerical resolution of the microstructured problem (3). The interfaces are discretized by an immersed interface method: see [26] and references therein for technical details.

The microstructured medium investigated here is similar to the one examined in [10], except that now it involves also the parameter γ_h in (3). As an example, let us take $h = 20$, with a phase A of length 5, and a phase B of length 15. The physical parameters are piecewise constant in each phase:

$$(\rho,\, E,\, \gamma) = \begin{cases} (1000,\, 10^9,\, 10^6) & \text{in phase A,} \\ (1500,\, 6\times 10^9,\, 10^6) & \text{in phase B.} \end{cases}$$

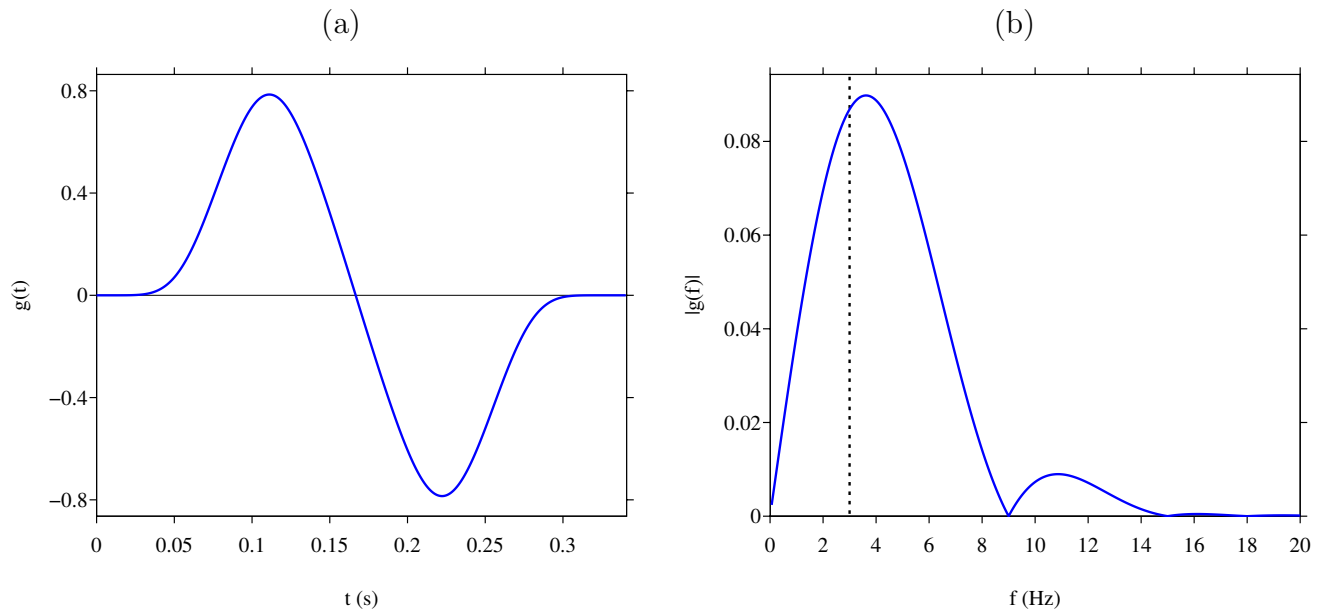

Figure 4: Time evolution of the source g (a) with a central frequency $f_c = 3$ and frequency evolution of the Fourier transform $|g(f)|$ (b). The vertical dotted line denotes f_c.

The effective parameters are $\rho_0 \approx 1375$, $E_0 \approx 2.66 \times 10^9$ and $\gamma_0 = 10^6$. It follows the effective phase celerity $c_0 = \sqrt{E_0/\rho_0} \approx 1392.62$. The physical domain [0, 1000] is discretized on 1000 grid nodes, hence $\Delta x = 1$.

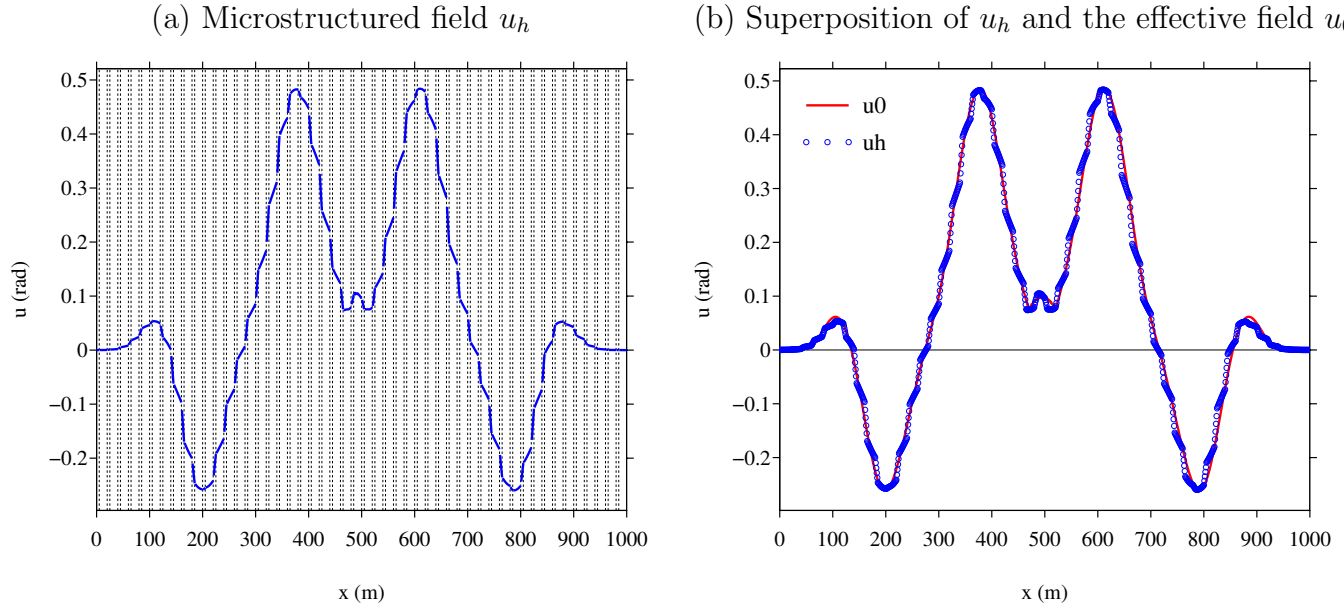

Figure 5: Snapshots of the fields at $t = 0.35$ emitted by a source point with central frequency $f_c = 3$ (i.e. $\eta_c = 0.043$). In (a), the dotted vertical lines denote the interfaces in the microstructured medium.

A source term $s(x, t)$ is introduced in the right-hand side of (3) or (15). This forcing is a

source point $s(x,t) = g(t)\,\delta(x - x_s)$ where g is a smooth combination of bounded sinusoids

$$g(t) = \begin{cases} G \sum_{m=1}^{4} a_m \, \sin(b_m \omega_c t) & \text{if } 0 < t < \dfrac{1}{f_c}, \\ 0 \;\; \text{otherwise,} \end{cases} \tag{53}$$

where $b_m = 2^{m-1}$, the coefficients a_m are $a_1 = 1$, $a_2 = -21/32$, $a_3 = 63/768$, $a_4 = -1/512$, and the amplitude factor G. It entails that g is a smooth function ($g \in C^6([0, +\infty[)$). Moreover, $g(t)$ is a wide-band signal with a central frequency $f_c = \omega_c/2\pi$ (Figure 4). This frequency is used to define a dimensionless parameter characteristic of the low-frequency regime underlying the formal asymptotic expansions used throughout the paper:

$$\eta_c = h\, f_c/c_0. \tag{54}$$

The source point is located at $x_s = 495$ in the middle of phase B. The amplitude is $G = \pi/4$.

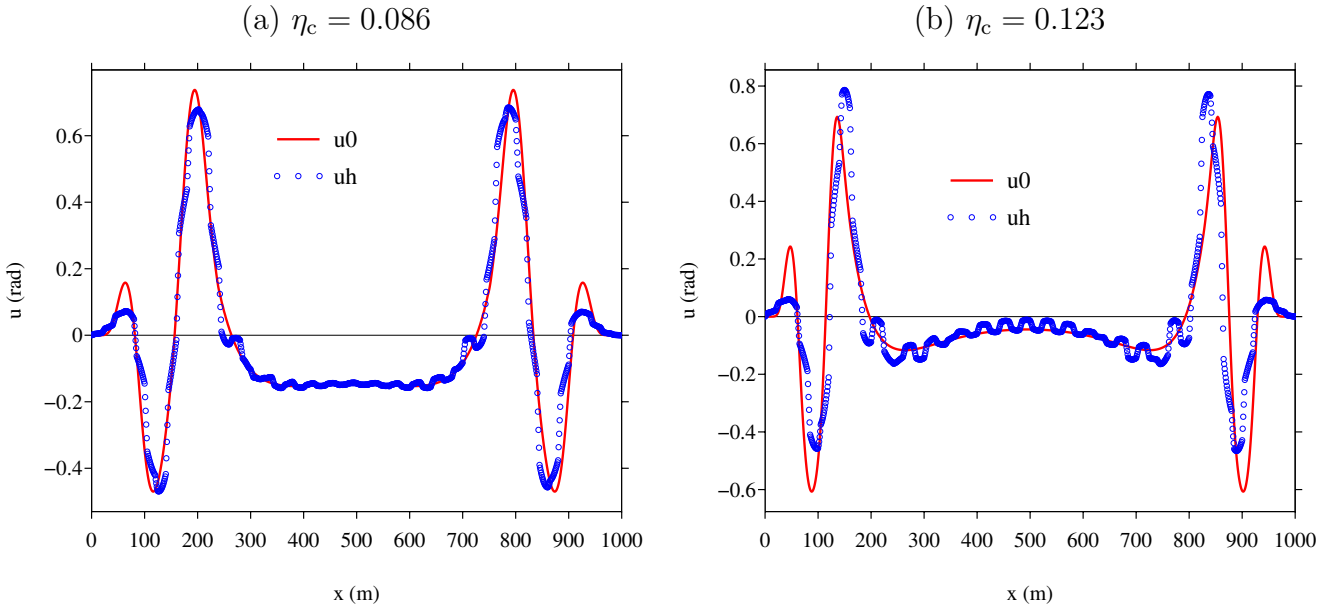

Figure 6: Superpositions of the microstructured field u_h and of the leading-order field u_0 at $t = 0.35$ for a central frequency $f_c = 6$ ($\eta_c = 0.086$) and $f_c = 9$ ($\eta_c = 0.123$).

Results. Figure 5 illustrates the low-frequency regime, with $f_c = 3$ (i.e. $\eta_c = 0.043$). A snapshot of u_h is shown at $t = 0.35$ (a). The vertical dotted lines indicate the interfaces between phases A and B. The source point in the middle of the domain emits left-going and right-going waves. Due to the symmetry of the problem, these waves are symmetrical with respect to x_s.

In contrast to [10], oscillations due to the dispersion of the sine-Gordon equation are observed. In (b), we compare u_h and u_0. The leading-order field u_0 captures well the mean value of u_h. On the other hand, the oscillations of u_h on the micro-scale are obviously not taken into account. To capture them, one would need to compute first-order correctors [6].

Figure 6 compares u_h and u_0 for higher frequencies. Logically, the agreement between the two fields deteriorates. In particular, additional oscillations due to the microstructure are not captured by the leading-order homogenization. To take them into account, the homogenization should be pushed to the second order [10].

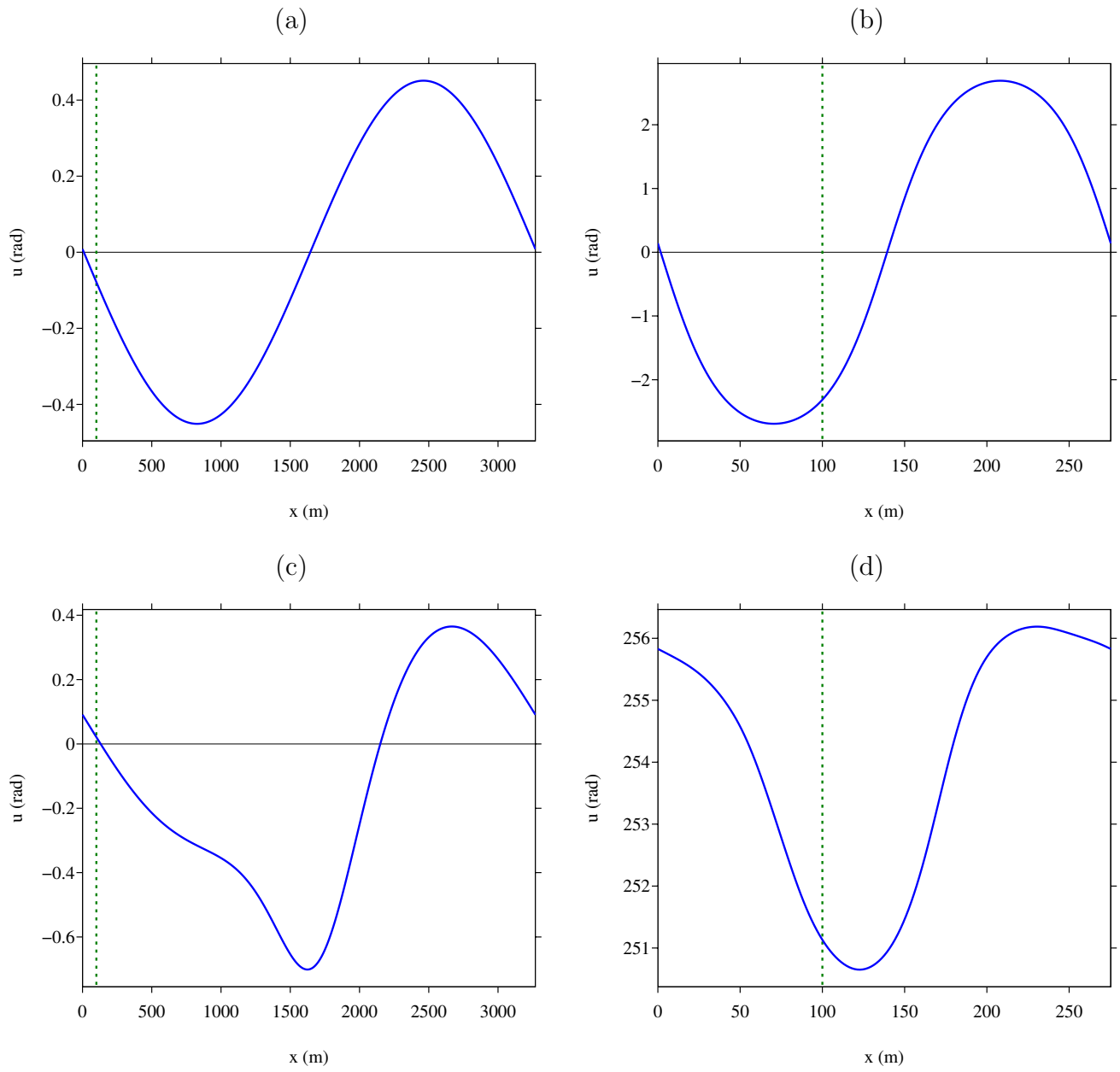

Figure 7: Snapshots of periodic solutions. Left column (a-c): $\mathcal{E} = 0.1$ and $D = 10$; right column (b-d): $\mathcal{E} = 1.9$ and $D = 1.1$. Top: initial data (a-b); bottom (c-d): solution at $t = 70$. The vertical dashed line refers to the position x_r of the receiver.

5.2. Periodic solutions

Set-up. From now on, we consider constant coefficients ρ_0, E_0 et γ_0 corresponding to the effective parameters of the Section 5.1. The propagation of periodic supersonic waves is investigated in two limit-cases: (i) $\mathcal{E} = 0.1$ and $D = 10$ (low energy and high speed $|D - 1|$); (ii) $\mathcal{E} = 1.9$ and $D = 1.1$ (high energy and low speed $|D - 1|$). In these two cases, the wavelengths are $\lambda \approx 3269.90$ and $\lambda \approx 275.29$, respectively.

The computations are initialized by a single period on a domain of length $L = \lambda$. The construction of the initial data is described in Section 3.3. Periodic boundary conditions are

implemented. Lastly, a receiver at $x_r = 100$ records u at each time step.

Results. Figure 7 shows the initial data and the solution after propagation. In the low-energy regime, the solution is difficult to distinguish from a sine (a), unlike in the high-energy regime (b). After propagation, we observe that both solutions are completely distorted (c-d), which highlights the instability of periodic solutions.

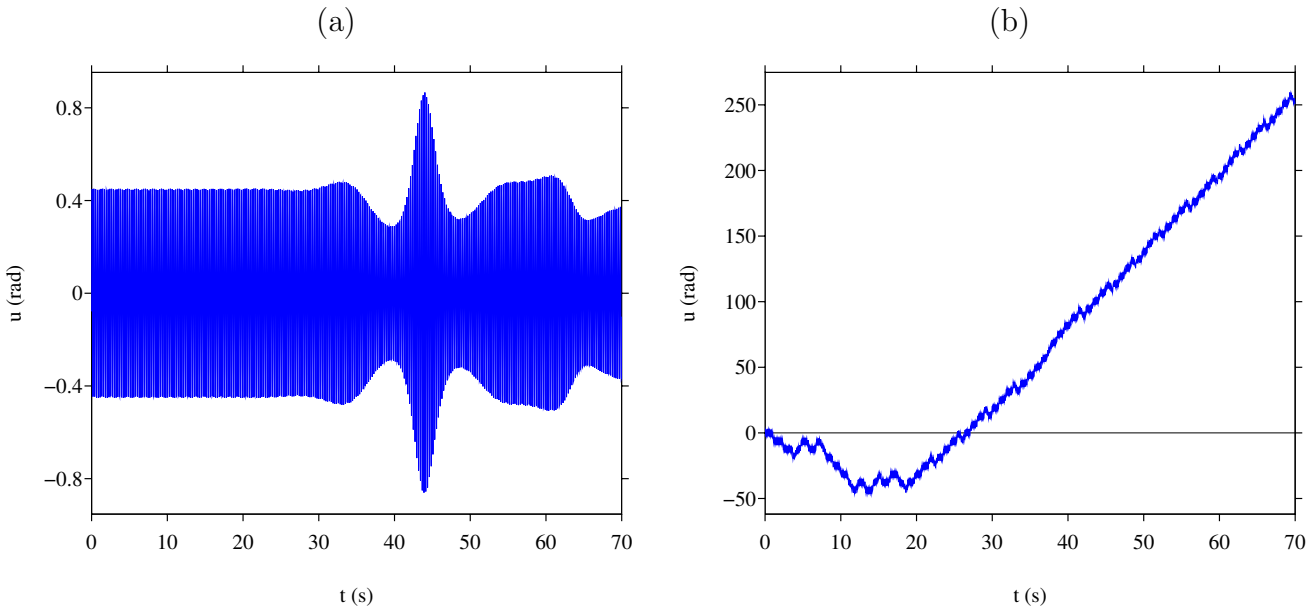

Figure 8: Time history of periodic solutions measured at the receiver. (a): $\mathcal{E} = 0.1$ and $D = 10$; (b): $\mathcal{E} = 1.9$ and $D = 1.1$.

Figure 8 shows the time history of $u(t, x_r)$. In the low-energy regime (a), the periodic solution destabilizes around $t = 30$ s. In the high-energy regime (b), we observe a succession of plateaus (at multiples of 2π) followed by a phase of approximately linear growth or decay. Similar numerical experiments have been carried out with $N > 1$ periods, i.e. on larger computational domains. The results are qualitatively the same as for $N = 1$, even if the details vary (e.g. time of instability).

5.3. Modulation equations

Set-up. The objective here is to illustrate numerically the findings of Section 4.4, where a scenario describing the instability of low-energy periodic solutions has been proposed. For this purpose, we consider a domain $[-L/2, L/2]$ and a even modulated energy $\mathcal{E}$, with a maximal energy $\overline{\mathcal{E}} = 0.1$ at $x = 0$; the speed, on the other hand, is maintained constant at $D = 10$ (supersonic wave). From (43) and (46), one chooses $a^2 = \overline{\mathcal{E}}/8$ so that

$$\mathcal{E}(x) = \overline{\mathcal{E}}\,\mathrm{sech}^2\left(\frac{x}{\Lambda}\right). \tag{55}$$

Based on $\mathcal{E}(x)$, D, and the algorithm described in Section 3.3, we construct the spatially modulated initial data $u(0, x)$ and the initial time derivative $u_t(0, x)$. At the origin, the amplitude of the initial data is $u(0, 0) \approx 0.45$. The wavelength for $(\overline{\mathcal{E}}, D)$ is $\overline{\lambda} \approx 3269.90$.

When moving away from $x = 0$, then the energy $\mathcal{E}$, the wavelength λ and the amplitude of $u(0, x)$ decrease, as deduced from (55) and from Figure 2. Contrary to the unmodulated case, the condition $u(0, L/2) = u(0, -L/2)$ (and similarly for u_t) is thus not automatically satisfied by choosing $L = N\overline{\lambda}$, where N is the number of archs. To enforce this condition while having N archs, then a iterative algorithm is implemented to determine L. Once done, periodic boundary conditions are applied for time-marching.

In line with the Whitham analysis, the envelope of u must be slowly varying, i.e. $\Lambda \gg \overline{\lambda} \geq \lambda$. We choose $\Lambda = 3 \times 10^4 \approx 10\,\overline{\lambda}$, so that the small parameter in (25) is $\mu = 0.1$. To be consistent with the ASK analytical solution (Section 4.4), the domain must also be sufficiently broad for mimicing an infinite domain. We choose $N = 40$ archs, so that $L \approx 1.29\,10^5$ and $\mathcal{E}(\pm L/2)/\overline{\mathcal{E}} = 0.052 \ll 1$. The modulation enveloppe and the initial data are displayed in Figure 9.

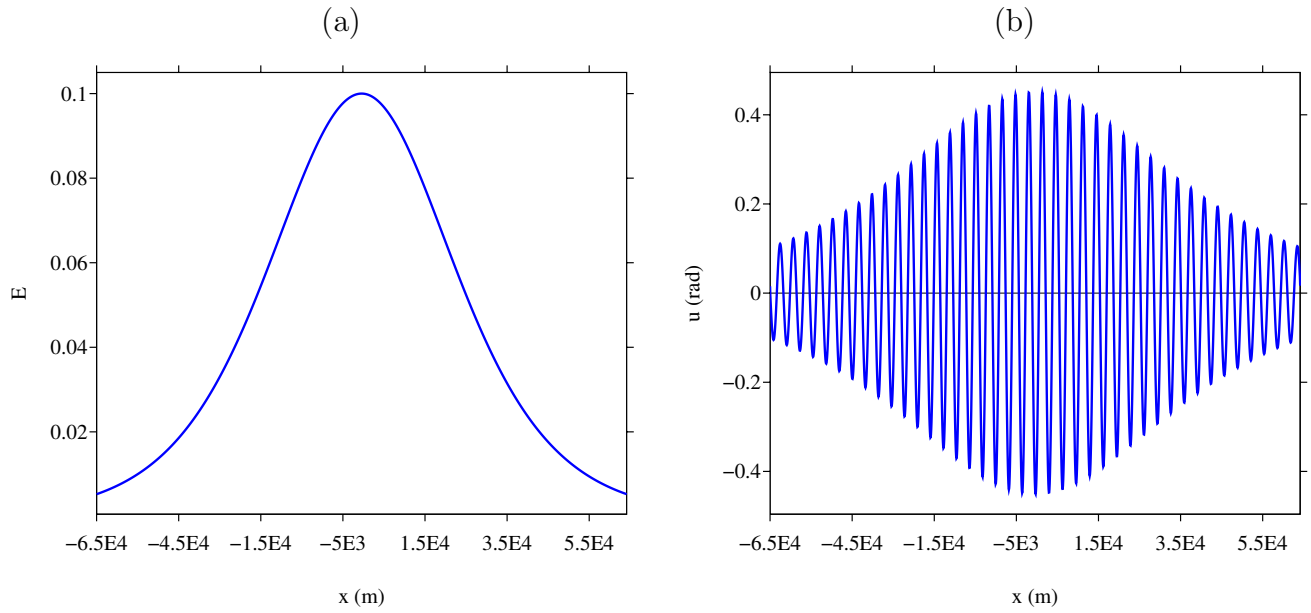

Figure 9: Modulation equation. (a): spatial evolution of $\mathcal{E}(x)$ in (55); (b): initial data $u(0, x)$.

Results. Figure 10-(a) shows a snapshot of u at $t = 20$. We observe that the maximum of u is always at the middle of the domain. The shape of the solution has changed, and the amplitude of $u(20, 0)$ is about 0.9, which corresponds roughly to a doubling of amplitude.

Figure 10-(a) shows the time evolution of $m(t) = \max_t(u)(t)$, where the maximum is taken at each instant over the whole computational domain. From the initial amplitude $m(0) \approx 0.45$, we observe that $m(t)$ oscillates and globally increases, reaching an maximum around 0.96 at $t = 21.5$, and then decreases. It is consistent with the analysis of Section 4.4, where the emergence of a caustic was predicted at $t_c = \Lambda/c_0 \approx 21.55$.

6. Conclusion

This work opens several research directions. A first direction is the theoretical study of the stability of periodic solutions for other regimes. In the high energy case, numerical observations

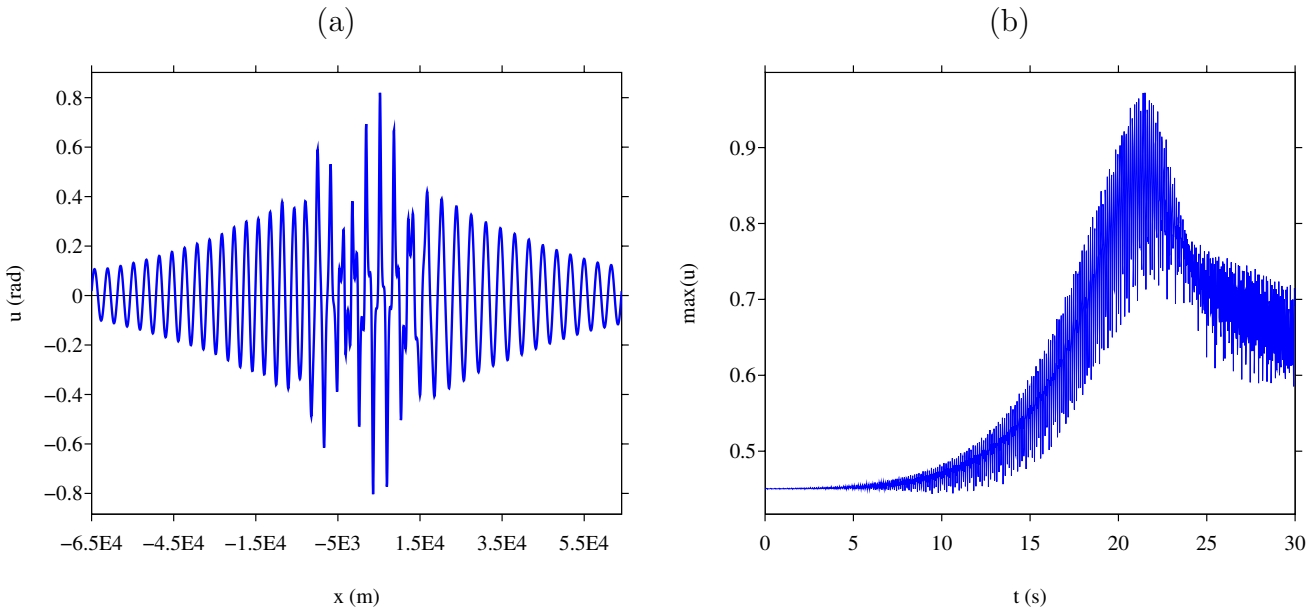

Figure 10: Modulation equations. (a): snapshot of u at $t = 20$. (b): time history of $\max_t(u)$.

have shown the existence of a linear evolution (Figure 8). This property remains to be studied theoretically.

A second direction is the high-order homogenization of the sine-Gordon equation with periodic coefficients. Following the energy approach outlined in Section 2, additional terms will be introduced into the effective equation. It would be interesting to understand whether the additional terms modify the stability properties of the corresponding modulation equations.

Appendix A. Proof of Lemma 1

Introducing $s^2 = \mathcal{E}/2$, one has

$$\begin{aligned} f(\mathcal{E}) &= g(s) = \frac{8\,s}{\pi}\int_0^{\arcsin(s)} \sqrt{1 - 1/s^2\sin^2\theta}\,d\theta, \\ &= \frac{8}{\pi}\int_0^{\arcsin(s)} \sqrt{s^2 - \sin^2\theta}\,d\theta. \end{aligned}$$

Let $t = \sin\theta$, then

$$g(s) = \frac{8}{\pi}\int_0^s \frac{\sqrt{s^2 - t^2}}{\sqrt{1 - t^2}}\,dt.$$

Now, let $t = s\,p$, then

$$g(s) = \frac{8\,s^2}{\pi}\int_0^1 \frac{\sqrt{1 - p^2}}{\sqrt{1 - s^2p^2}}\,dp.$$

Introducing $p = \sin\varphi$, one has

$$\begin{aligned} g(s) &= \frac{8\,s^2}{\pi}\int_0^{\pi/2} \frac{\cos^2\varphi}{\sqrt{1 - s^2\sin^2\varphi}}\,d\varphi, \\ &= \frac{8(s^2-1)}{\pi}\int_0^{\pi/2} \frac{d\varphi}{\sqrt{1 - s^2\sin^2\varphi}} + \frac{8}{\pi}\int_0^{\pi/2} \sqrt{1 - s^2\sin^2\varphi}\,d\varphi. \end{aligned}$$

Let $s^2 = m$, then $m = \mathcal{E}/2$ and

$$\begin{aligned} f(\mathcal{E}) &= h(m) = \frac{8(m-1)}{\pi} \int_0^{\pi/2} \frac{d\varphi}{\sqrt{1 - m\,\sin^2\varphi}} + \frac{8}{\pi} \int_0^{\pi/2} \sqrt{1 - m\,\sin^2\varphi}\, d\varphi, \\ &= \frac{8(m-1)}{\pi}\, K(m) + \frac{8}{\pi} E(m), \end{aligned}$$

with K and E are the complete elliptic integrals of the first kind and second kind, respectively. These integrales satisfy the properties

$$E^{'}(m) = \frac{1}{2m}\left(E(m) - K(m)\right), \qquad K^{'}(m) = \frac{1}{2m(1-m)}\left(E(m) - (1-m)\,K(m)\right).$$

It follows

$$f^{'}(\mathcal{E}) = \frac{2}{\pi}\, K\left(\frac{\mathcal{E}}{2}\right)$$

and the expression of $f^{''}(\mathcal{E})$. A Taylor expansion of f around the origin gives

$$f(\mathcal{E}) = \mathcal{E} + \frac{1}{16}\,\mathcal{E}^2 + \frac{3}{256}\,\mathcal{E}^3 + \frac{25}{8192}\,\mathcal{E}^4 + \cdots ...$$

and thus

$$\lim_{\mathcal{E}\to 0^+} f^{'}(\mathcal{E}) = 1,$$

which concludes the proof.

References

[1] M. Abramowitz and I. Stegun, *Handbook of Mathematical Functions with Formulas, Graphs, and Mathematical Tables*, National Bureau of Standards Applied Mathematics Series, No. 55, U. S. Government Printing Office, Washington, 1964.

[2] S. A. Akhmanov, A. P. Sukhorukov, and R. V. Khokhlov, Zh. Eksp. Teor. Fiz. 50, 1537 (1966) [Sov. Phys. JETP, 23, 1025 (1966)].

[3] G. Allaire, *Homogenization and two scale convergence*, SIAM J. Math. Anal. 23 (1992), 1482–1518.

[4] G. Allaire, A. Lamacz and J. Rauch, *Crime pays; homogenized wave equations for long times*, Asymptotic Analysis Asymptotic Analysis 128-3 (2022), 295-336.

[5] S. Baker, and N. F. Smyth, Modulation theory and resonant regimes for dispersive shock waves in nematic liquid crystals, **403** 132334 (2020)

[6] C. Bellis, B. Lombard, M. Touboul, R. Assier, *Effective dynamics for low-amplitude transient elastic waves in a 1D periodic array of non-linear interfaces*, Journal of the Mechanics and Physics of Solids 149 (2021), 104321.

[7] T. B. Benjamin, J. L. Bona and J. J. Mahony, 1972 *Model equations for long waves in nonlinear dispersive systems*, Phil. Trans. Royal Soc. A 272 (1972), 47–78.

[8] S. Benzoni-Gavage, C. Mietka and L.M. Rodrigues, *Modulated equations of Hamiltonian PDEs and dispersive shocks*, Nonlinearity 34 (2021), 578-641.

[9] T. J. Bridges, *Symmetry, Phase modulation and Nonlinear Waves*, Cambridge Monographs on Applied and Computational Mathematics, Cambridge, 2017

[10] R. Cornaggia, B. Lombard, *An homogenized model accounting for dispersion, interfaces and source points for transient waves in 1D periodic media*, ESAIM: Mathematical Modelling and Numerical Analysis 57 (2023), 1413-1444.

[11] A.L. Dalibard, *Homogenization of nonlinear scalar conservation laws*, Archive for Rational Mechanics and Analysis 192-1 (2009), 117-164.

[12] T. Dauxois and M. Peyrard, Physics of Solitons, Cambridge University Press, Cambridge, 2010.

[13] B. Dubrovin, T. Grava, C. Klein, *On universality of critical behaviour in the focusing nonlinear Schrödinger equation, elliptic umbilic catastrophe and the tritronquée solution to the Painlevé-I equation*, J. Nonlinear Sci. 19 (2009), 57-94.

[14] El G A, Grimshaw R H J and Smyth N F 2006 Unsteady undular bores in fully nonlinear shallow-water theory, Phys. Fluids **18** 027104.

[15] El G A and Hoefer M 2016 Dispersive shock waves and modulation theory, Physica D **333** 11-65.

[16] S. Gavrilyuk, K.M. Shyue, *Singular solutions of the BBM equation: analytical and numerical study*, Nonlinearity 35-1 (2022), 388.

[17] A. V. Gurevich, A. V. Krylov and G. A. El, *Nonlinear modulated waves in dispersive hydrodynamics*, J. Exp. Theor. Phys 98 (1990), 1605–1626.

[18] A. V. Gurevich, L. P. Pitaevskii, *Nonstationary structure of a collisionless shock wave*, JETP 38 (1974), 291– 297.

[19] M.A. Johnson, W.R. Perkins, *Modulational instability of viscous fluid conduit periodic waves*, SIAM Journal on Mathematical Analysis 52-1 (2020).

[20] C.K.R.T. Jones, R. Marangell, P.D. Miller and R.G. Plaza, *Spectral and modulational stability of periodic wavetrains for the nonlinear Klein-Gordon equation*, J. Differential Equations 257 (2014), 4632-4703.

[21] A. M. Kamchatnov, *Nonlinear Periodic Waves and Their Modulations: An Introductory Course*, World Scientific Publishing, 2000.

[22] A. M. Kamchatnov and D. V. Shaykin, *Propagation of instability fronts in modulationally unstable systems*, EPL 136 (2021), 40001.

[23] A. M. Kamchatnov, *Modulation theory for the sine-Gordon equation*, https://arxiv.org/abs/2301.04360 (2023).

[24] D. I. Ketcheson and R. J. LeVeque, *Shock dynamics in layered periodic media*, Communications in Mathematical Sciences 10 (2012), 859–874.

[25] A. C. Scott *A Nonlinear Klein-Gordon Equation*, American Journal of Physics 37 (1969), 52.

[26] M. Touboul, B. Lombard, C. Bellis, *Time-domain simulation of wave propagation across resonant meta-interfaces*, Journal of Computational Physics 414-1 (2020), 109474.

[27] A. Wautier and B.B. Guzina, *On the second-order homogenization of wave motion in periodic media and the sound of a chessboard*, Journal of the Mechanics and Physics of Solids 78 (2015), 382–414.

[28] G. B. Whitham, *Non-linear dispersive waves*, Proc. Roy. Soc. London 283 A (1965), 238–291.

[29] G. B. Whitham, *Linear and Nonlinear Waves*, John Wiley and Sons, 1974.